

Removal and determination of carbon monoxide based on copper oxide immobilized on Zeolite 13X Nanocatalyst by catalytic oxidation process and gas flow analyzer

Bahar Parsazadeh^a, Hasan Asilian Mahabadi^{a,*}, and Niloofar Damyar^b

^aDepartment of Occupational Health, Faculty of Medical Sciences, Tarbiat Modares University, Tehran, Iran

^bDepartment of Occupational Health, Damghan School of Public Health, Semnan University of Medical Sciences, Semnan, Iran

ARTICLE INFO:

Received 2 Aug 2023

Revised form 14 Oct 2023

Accepted 3 Nov 2023

Available online 28 Dec 2023

Keywords:

Carbon monoxide,
Copper Oxide nanoparticles,
Zeolite 13X,
Catalytic oxidation,
Response surface methodology,
Central composite design

ABSTRACT

Carbon monoxide is one of the main air pollutants, mainly produced from the incomplete combustion of fossil fuels. This study aims to oxidize carbon monoxide by copper oxide nanoparticles immobilized on zeolite13X substrate. The present investigation was conducted to determine the effect of carbon monoxide concentration parameters (in the range of 200-1400 ppm) and reaction temperature (in the range of 100-500 °C) on the efficiency of carbon monoxide conversion by CuO/Zeolite 13X nanocatalyst. The design of the experiment and the determination of the number of experiments were analyzed using the central composite design method, and the statistical test of analysis of variance was done using the response surface method. Also, the structural and morphological characteristics of the nanocatalyst were investigated using BET, BJH, FE-SEM, EDX, and XRF tests. The results show that CuO/Zeolite 13X nanocatalyst efficiently oxidizes carbon monoxide. The highest conversion efficiency of 82.6% was obtained at a temperature of 400 °C and a carbon monoxide concentration of 500 ppm as the optimal conditions. According to the EDX test results, copper oxide nanoparticles with a weight percentage of 5.9% were loaded on the Zeolite 13X substrate. Design Expert11 software reduced the cubic model with an R_2 coefficient of 0.98.

1. Introduction

According to the World Health Organization (WHO), 7 million deaths occur yearly due to air pollution [1]. Carbon monoxide is a colourless,

odourless, and non-irritating gas mainly produced from the incomplete combustion of carbonaceous materials (coal, diesel, natural gas, oil, propane, and so forth) [2]. Industries and vehicles are the most important sources of this gas emission [3]. Carbon monoxide is a poisonous gas for humans and animals and also has adverse effects on the environment [2] Regarding the concentration

*Corresponding Author: [Hasan Asilian Mahabadi](mailto:Hasan.Asilian.Mahabadi@modares.ac.ir)

Email: asilian_h@modares.ac.ir

<https://doi.org/10.24200/amecj.v6.i04.259>

of carbon monoxide in the exhaust air of Iran's industries, several investigations have been carried out, for example, in 2010, Junadi et al. investigated the exhaust of waste incinerators of several hospitals in Hamedan city, and the highest concentration of carbon monoxide reported as 1041 ppm, which 10.4 times the standard of the Environmental Organization in 2002 [4]. Also, in another study, Guderzi et al. investigated the pollutants from cement industries in Lorestan city, and based on the results, the highest concentration of carbon monoxide is related to winter and spring seasons and is equal to 630 ± 53.04 and 2378 ± 76 ppm, respectively, which are higher than the permissible exposure limit [5]. About 95% of the absorbed carbon monoxide is easily combined with hemoglobin to form carboxyhemoglobin. Complications such as muscle paralysis, coma, cardiovascular complications, and eventual death occur when the percentage of carboxyhemoglobin increases by more than 50%. Also, nano-palladium embedded on the mesoporous silica nanoparticles was used for CO and mercury removal from air [2, 6]. Hence, controlling and reducing the concentration of carbon monoxide is essential in maintaining public health. Oxidation of carbon monoxide to carbon dioxide is a practical and straightforward way to control this pollutant [7]. Using heterogeneous catalysts to oxidate various chemical compounds is among the leading technologies in advanced environmental science and engineering [8-10]. Many studies have reported that platinum group metals (PGM), including Platinum (Pt), Palladium (Pd), Radium (Rd), and Iridium (Ir), have high catalytic activity for carbon monoxide oxidation [11, 12]. However, their use as catalysts is limited due to challenging problems such as low natural abundance, high cost, and sulphur poisoning [13]. Therefore, transition metals such as copper [14, 15], nickel [16, 17] and cobalt [18] and their combinations have been considered for carbon monoxide oxidation due to their high natural abundance and high stability [13, 14, 19, 20] To date, many studies have been performed to investigate the catalytic activity of nanocatalysts.

According to previous studies, metal nanoparticles used as catalysts can help improve the reaction efficiency due to their high surface-to-volume ratio, specific surface area, and high chemical and thermal resistance [21, 22]. Hence, attempts have been made to place active nanostructures on mesoporous supports to increase the stability of nanocatalysts and prevent them from c. So far, various porous materials, such as metal oxides, diatomite, zeolites, activated carbon, and alumina, have been studied to make copper oxide catalysts [23-27]. Zeolites are available in synthetic and natural forms and generally consist of a basic structure consisting of an aluminosilicate framework and a quadrilateral set of silicate cations (SiO_4^+) and aluminum (Al^{3+}) cations surrounded by four oxygen anions. Synthetic zeolites have a higher surface area, more pore volume, and no impurities compared to natural zeolites [28, 29]. NaX faujasite (with the brand name of zeolite 13X) is an alkaline metal aluminosilicate with the sodium form of zeolite X [30, 31]. However, the investigation of the catalytic activity of copper oxide nanoparticles immobilized on zeolite 13X was not found by our research team.

This study aimed to catalyze carbon monoxide oxidation by zeolite 13X stabilized copper oxide nanocatalyst. The CCD central composite design method (a subset of the RSM response surface method) and the Design-Expert software version 11 were used to design, model, and optimize the experiments.

2. Experimental

2.1. Catalyst preparation

This study synthesized the copper oxide using aqueous copper acetate salt $\text{Cu}(\text{OAc})_2 \cdot \text{H}_2\text{O}$ by co-precipitation. Previous research reported 4-5% by weight of copper oxide fixed on the support as the optimal catalyst [20, 32]. Accordingly, CuO/Zeolite 13X nanocatalyst with 4% by weight was investigated in this study. To make a copper oxide nanocatalyst of 4% by weight, 2.8 g of the aqueous copper acetate salt ($\text{Cu}(\text{OAc})_2 \cdot \text{H}_2\text{O}$) was added to 100 cc of distilled water to reach a clear blue solution. The solution temperature was adjusted to 80 °C, and

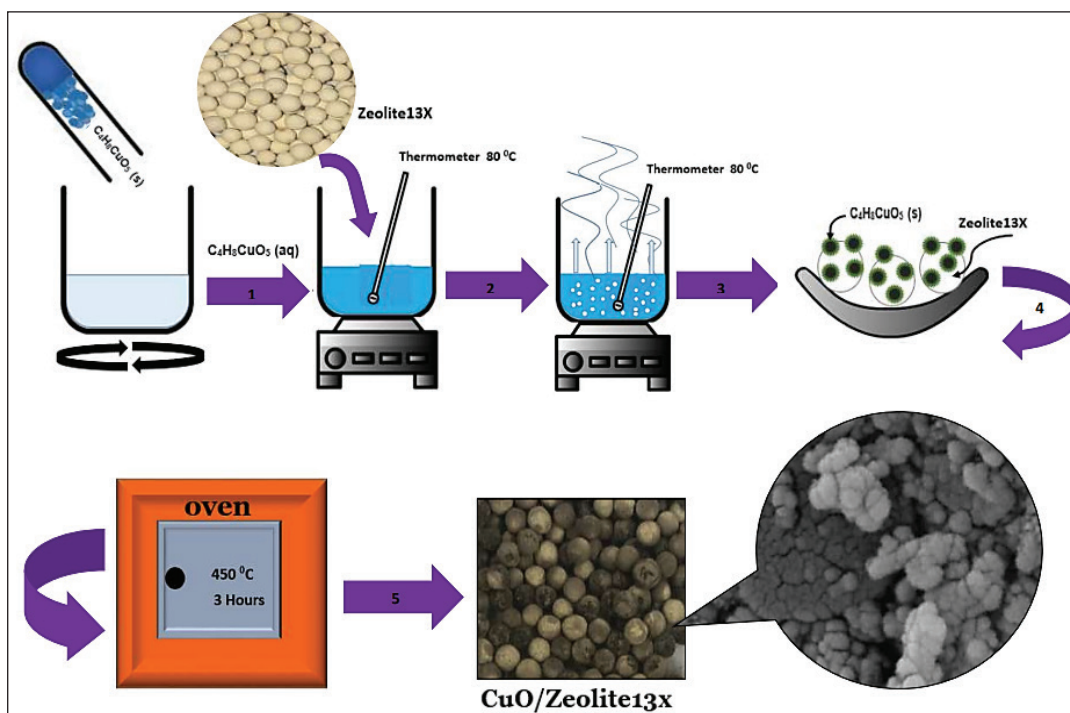


Fig. 1. Schematic view of the manufacturing steps of CuO/Zeolite13X nanocatalyst

20 g of zeolite 13X was added. The suspension was then placed on a mixer and gently stirred until all the water in the suspension was evaporated. Next, zeolite pellets impregnated with copper acetate salt were calcined at 450 °C for 3 hours (Fig.1).

2.2. Characterization

Elemental analysis of zeolite13x was performed by X-ray fluorescence test (XRF) using an XRF device (model PW 2404 Philips Company) with the LIO method (loss-on-ignition) on pressed powders. The Brunauer-Emmett-Teller (BET) and Barrett-Joyner-Halenda (BJH) tests determined specific surface area, pore volume, and pore size. The tests were performed with the physical adsorption of N₂ at -196 °C using a micrometric TriStar II 3020 analyzer. Field Emission Scanning Electron Microscope (FE-SEM) and Energy-dispersive X-ray spectroscopy (EDX) examined the morphology of the catalyst and quantitative and elemental identifications appended with FE-SEM, respectively. Using FE-SEM analysis, high-resolution images of the catalyst surface were provided with a magnification of 5,000 x and an operating voltage of 20 kV.

2.3. Procedure based on catalytic activity and gas flow analyzer

Catalytic activity tests of copper oxide nanocatalysts were performed in a fixed bed reactor (quartz glass tube with an inner diameter of 13 mm and a catalyst length of 20 mm were used) at the atmospheric pressure and with a 1 liter per minute flow rate. As shown in Figure 2, a carbon monoxide cylinder with a purity of 99.99% was used as the main gas, and purified ambient air (silica gel and soda-lime) was used as the carrier gas. The concentration of carbon monoxide was adjusted by needle valves, rotameters, and flowmeters with control valves in the path before the reactor, and its amount was determined both before and after the reactor (reactor outlet) by a continuous gas flow analyzer (MRU Vario Plus, Germany) with 10-ppm accuracy which was calibrated before all tests. This device is Suitable for industrial applications using combined infrared (NDIR) technology and electrochemical sensors for maximum versatility. It can measure 9 gases, including O₂, CO, NO, NO₂, NO_x, SO₂, CO-high, CO-very high, H₂S or H₂, CH₄ or C₃H₈. This device can measure carbon monoxide, carbon dioxide, and oxygen simultaneously. To perform the tests, the supported copper oxide nanocatalyst was

placed in an oven at 150 °C for 2 hours with the aim of dehumidifying, and then 1 g of it was placed in a reactor (Fig.3). Refractory fibreglass was also used to hold the catalysts in place. The conversion efficiency of carbon monoxide to carbon dioxide was calculated by Equation 1.

$$\eta\% = \frac{C_{in} - C_{out}}{C_{in}} \times 100$$

(Eq. 1)

In this equation: C_{in} : input concentration (ppm), C_{out} : output concentration (ppm), and η : efficiency in percentage.

2.4. Experimental design and statistical analysis

To achieve maximum efficiency, there is a need to optimize the process variables. Traditional and old optimization methods are done by considering the effect of a parameter on the process at a certain time. In recent years, to overcome the shortcomings, the

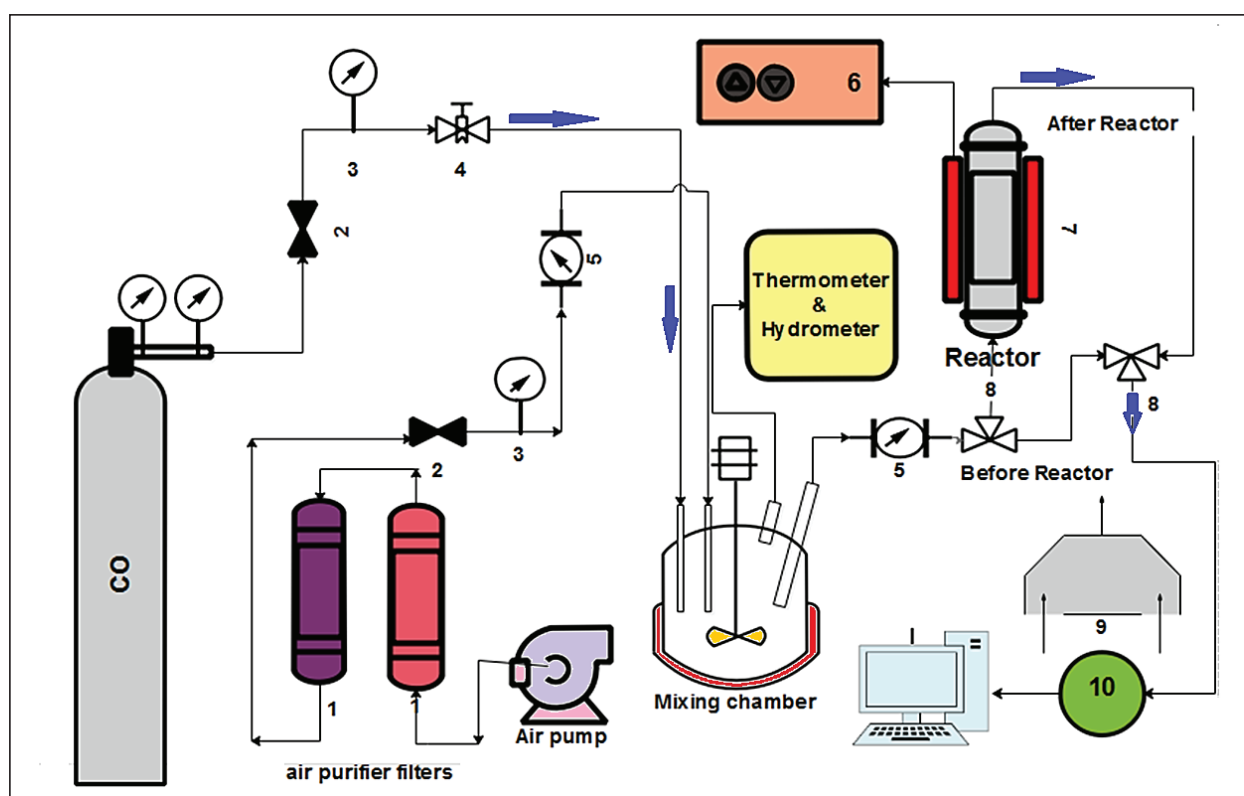


Fig. 2. Schematic design of the test set-up, 1: Gas valves, 3: Pressure measurement, 4: Needle valve, 5: Flowmeter, 6: Heat control thermostat, 7: Furnace, 8: Three-way valve, 9: Vent, 10: Gas analyzer

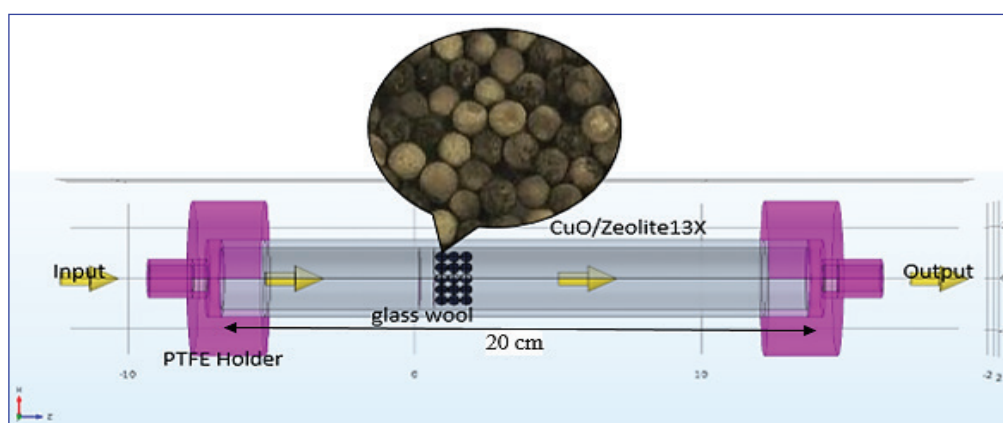


Fig. 3. The packed CuO/Zeolite 13X reactor

Table 1. The experimental range and levels of the factors in the CCD

Factor	Name	Units	Type	Minimum	Maximum	Coded low	Coded high	Mean
A	Temperature	°C	Numeric	100.00	500.00	-1 ↔ 200.00	+1 ↔ 400.00	300.00
B	Concentration	ppm	Numeric	200.00	1400.00	-1 ↔ 500.00	+1 ↔ 1100.00	800.00
C	packing type	Categoric		Zeolite13X	CuO/Zeolite13X			Levels: 2

RSM response surface method, which is a powerful optimization method, has been widely used [33-35]. This method is based on mathematical and statistical techniques that find optimal conditions by understanding the effects of various factors and their interaction on the response. CCD (Central Composite Design) is one of the most common RSM methods [36] [37]. As shown in Table 1, temperature variables and carbon monoxide concentration in 5 levels α , -1, 0, + α , +1 were examined. Also, the qualitative catalyst type variable was studied in CuO/Zeolite 13X and Zeolite 13X (uncoated catalyst base). After carrying out the carbon monoxide oxidation tests, the effect of each independent variable (carbon monoxide concentration and temperature) on the response and their relationship with each other was obtained by Equation 2 [38].

$$Y = \beta_0 + \sum_{i=1}^k \beta_i X_i + \sum_{i=1}^k \beta_{ii} X_i^2 + \sum_{i=1}^k \sum_{j=1}^k \beta_{ij} X_i X_j + e_{ij} \quad (\text{Eq.2})$$

In this formula, Y is the predicted response, β_0 is a constant coefficient, β_i is the linear effects, β_{ii} squared effect, β_{ij} interaction, e_{ij} random error, X_i and X_j are the temperature and concentration of carbon monoxide (independent variables), respectively.

3. Results and Discussion

3.1. Statistical analysis of the catalytic conversion of CO

This study aimed to determine the influential factors on carbon monoxide conversion efficiency (CEC), study the interaction of variables, and determine their optimal values. Table 1 lists the variables under consideration, which were reaction temperature (A) and CO concentration (B) under two reactors' conditions (reactor packed with Zeolite13X (uncoated base) and reactor packed with CuO/Zeolite13X nanocatalyst). The minimum and maximum values of

the main variables (CO gas concentration and reaction temperature) were selected according to the reported conditions of the exhaust gas concentration of many industries and refineries, according to the values given in Table 1. Firstly, CO adsorption by uncoated Zeolite 13X pellets was investigated to ensure that they had no adsorption and catalytic effects. The central composite design (CCD) method in 5 levels has been used to obtain logical results in this research. To evaluate the effect of variables, the reaction temperature (A), carbon monoxide gas concentration (B) and type of packed reactor (C), 26 tests were designed using the CCD method, and the results of each test are given in Table 2.

3.2. Model matching and statistical analysis

The experimental data from 26 runs defined by the CCD were analyzed to achieve significant and insignificant effects of each variable and their interactions. Then, the best regression model will be obtained to predict the carbon monoxide conversion efficiency of the reactor packed with CuO/Zeolite 13X and zeolite 13X. ANOVA results for the selected reduced cubic model, which can predict the response (carbon monoxide conversion efficiency), are given in Table 3. According to the obtained results (Table 2), the carbon monoxide conversion efficiency for the reactor packed with Zeolite 13X is 0.11-7.43%, which is significantly higher than that of the reactor packed with CuO/Zeolite 13X nanocatalyst. In this study, the maximum carbon monoxide conversion efficiency is achieved by CuO/Zeolite 13X nanocatalyst (92.96%), which is 12.5 times greater than that of the reactor packed with Zeolite 13X. Therefore, it can be concluded that Zeolite 13X is catalytically inactive, which is consistent with other studies conducted in this area. To achieve the carbon monoxide conversion efficiency (CEC) regression model, according to the results obtained from 26 tests, Equations 3 and 4 were created by Design-Expert software version 11.

Table 2. Results of CO conversion efficiency experiments

Run	A: Temperature (°C)	B: CO concentration (ppm)	C: Catalyst type	(%) $\eta_{\text{predicted}}$	(%) η_{actual}
1	300	800	ZeoliteX13	3.74	3.08
2	400	1100	ZeoliteX13	5.16	5.70
3	100	800	CuO/ZeoliteX13	2.31-	6.77
4	300	800	ZeoliteX13	3.74	3.10
5	300	200	ZeoliteX13	5.47	5.76
6	300	800	CuO/ZeoliteX13	46.85	41.57
7	300	1400	ZeoliteX13	2.02	2.10
8	300	800	ZeoliteX13	3.74	2.77
9	500	800	ZeoliteX13	8.31	9.10
10	300	800	ZeoliteX13	3.74	2.68
11	400	1100	CuO/ZeoliteX13	66.84	78.89
12	400	500	CuO/ZeoliteX13	76.02	82.60
13	200	500	CuO/ZeoliteX13	26.86	22.10
14	300	800	ZeoliteX13	3.74	3.13
15	300	800	CuO/ZeoliteX13	46.85	41.20
16	200	500	ZeoliteX13	2.32	2.50
17	300	1400	CuO/ZeoliteX13	37.67	38.02
18	200	1100	CuO/ZeoliteX13	17.68	16.81
19	300	800	CuO/ZeoliteX13	46.85	42.85
20	500	800	CuO/ZeoliteX13	96.01	92.96
21	100	800	ZeoliteX13	0.82-	0.11
22	400	500	ZeoliteX13	6.89	7.43
23	300	800	CuO/ZeoliteX13	46.85	42.05
24	200	300	CuO/ZeoliteX13	56.03	61.06
25	200	1100	ZeoliteX13	0.60	1.20
26	300	800	CuO/ZeoliteX13	46.85	42.20

The following equations can predict the CEC at the levels of the original units determined for each factor.

$$\begin{aligned} R\% \text{ CuO/Zeolite13X} = & +17.19889 \\ & +0.112493A-0.054183B+0.000013AB \\ & +0.000205A^2+0.000022B^2 \end{aligned} \quad (\text{Eq.3})$$

$$\begin{aligned} R\% \text{ Zeolite13X} = & +3.32835 \\ & +0.000295A-0.006330B-3.58333E-06AB \\ & +0.000042A^2+2.83118E-06B^2 \end{aligned} \quad (\text{Eq.4})$$

Analysis of variance (Table 3) showed that the selected reduced cubic model with P-values of less than 0.05 and a 95% confidence interval is suitable for predicting CEC. The factors of reaction temperature (A), CO concentration (B), packed reactor type (C),

and AC interaction) have P-values less than 0.05 and are significant factors in carbon monoxide conversion efficiency. This model is robust, with more than 99.99% accuracy. Based on the statistical results, the values predicted by the model with the results of regression experiments are equal to 0.98. Also, the R-square (R^2) and adjusted R-squared (adj, R^2) are equal to 0.98 and 0.97, respectively, with a difference of less than 0.2, indicating the model's suitability. The precision also shows the signal-to-noise ratio, which is 31.54 for the prediction model, which is more than four and is desirable. Also, the standard deviation values (SD) and the coefficient of variation (CV) equal 68.4 and 18.50, respectively. Based on these results, the predicted values and the values obtained from the experimental tests for the CO conversion efficiency

response have good regression, which indicates that this model can be used with good reliability to predict the response. Parameters A and B represent the actual reaction temperature and CO concentration values, respectively. Positive regression coefficients indicate a positive linear effect, and negative regression coefficients indicate a negative linear effect on carbon monoxide conversion efficiency. It should be noted that the P-value determines the effect of each parameter. For significant parameters, the smaller the P-value, the greater the effect of that parameter on the response, and if the P-values are the same, the F-value should be considered; the higher this value is, the greater the effect of the parameter on the response.

The significant parameters in this study based on their importance in carbon monoxide conversion efficiency are $C > A > AC > B$. The comparison of the predicted values obtained from the selected model against the actual values obtained from the experimental tests for the intended response is shown in Figure 4. The scatter of points around the diagonal line (Figure 4) shows a good correlation between the experimental data and the predicted values and, consequently, the model's strength. Based on these results, the predicted values and the values obtained from experiments for the CO conversion efficiency response showed a good regression, revealing that this model can be used with good reliability to predict the response.

Table 3. ANOVA for Reduced Cubic model

Source	Sum of Squares	df	Mean Square	F-value	p-value
Model	19803.02	11	1800.27	82.23	< 0.0001
A-Temperature	4330.10	1	4330.10	197.78	< 0.0001
B-Concentration	178.38	1	178.38	8.15	0.0127
C-Type of reactor	4647.60	1	4647.60	212.28	< 0.0001
AB	0.1653	1	0.1653	0.0076	0.9320
AC	2982.63	1	2982.63	136.23	< 0.0001
BC	83.37	1	83.37	3.81	0.0713
A ²	69.88	1	69.88	3.19	0.0957
B ²	56.45	1	56.45	2.58	0.1306
ABC	0.5050	1	0.5050	0.0231	0.8815
A ² C	30.17	1	30.17	1.38	0.2600
B ² C	33.51	1	33.51	1.53	0.2364

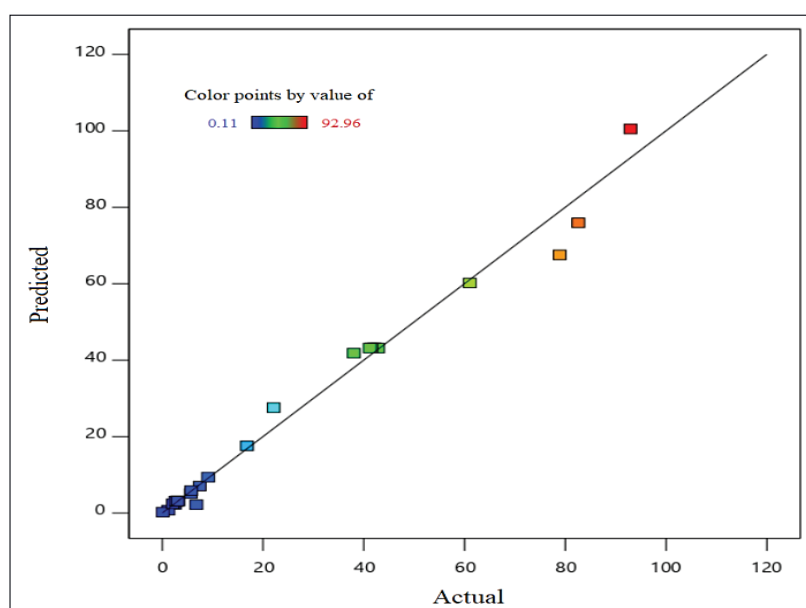


Fig. 4. Comparison of values predicted by the model and obtained from experimental tests

3.3. Effect of carbon monoxide concentration and reaction temperature on carbon monoxide conversion efficiency

The effect of the main parameters, i.e. reaction temperature and CO concentration, on carbon monoxide conversion efficiency is shown in Table 3. Based on the obtained results and as expected, there is a linear relationship between carbon monoxide conversion efficiency and reaction temperature, CO concentration, and type of reactor.

Figure 5a shows the carbon monoxide conversion efficiency by CuO/Zeolite 13X and Zeolite 13X nanocatalysts as a function of reaction temperature. The composition of the incoming feed stream contains 800 ppm of CO gas with a space velocity of 22641 h⁻¹. Based on the analysis of variance, reaction temperature (A) has a positive linear effect on carbon monoxide conversion efficiency. According to the results shown in Figure 5a, the CuO/Zeolite 13X nanocatalyst is inactive at temperatures below 100°C, and the carbon monoxide conversion efficiency is low. At a temperature of 100 °C, the conversion efficiency is equal to 6.77% (experiment number 3) and with increasing temperature, the efficiency of carbon monoxide conversion also increases so that it reaches 41.57% on average at a temperature of 300°C and 92.96% at a temperature

of 500 °C (experiment number 20) found that the obtained results are consistent with similar studies [20, 32]. Of course, according to previous studies [39], by using copper oxide nanoparticles with a smaller diameter (up to 5 nm), it is possible to achieve a carbon monoxide conversion efficiency of 99.5% at a temperature of 250 °C, which indicates the effect of the catalyst preparation method and the size of the nanoparticles.

Figure 5b shows the effect of CO concentration of 1100-500 ppm on CEC during carbon monoxide oxidation by CuO/Zeolite13X and Zeolite13X nanocatalysts at 300°C and with a space velocity of 22641 h⁻¹. Based on the analysis of variance, CO concentration has a linear negative effect on carbon monoxide conversion efficiency. The experimental results show that when the concentration of CO is equal to 500 and 1100 ppm at a constant temperature of 400 °C, the conversion efficiency of carbon monoxide is equal to 82.60% (experiment number 12) and 78.89% (experiment number 11), respectively. Theoretically, the conversion efficiency decreases with the increase in pollutant concentration, which is consistent with the results of this study. Of course, using a pure oxygen cylinder can limit this effect and increase the catalyst's efficiency [40], which could not be used in this study due to existing limitations.

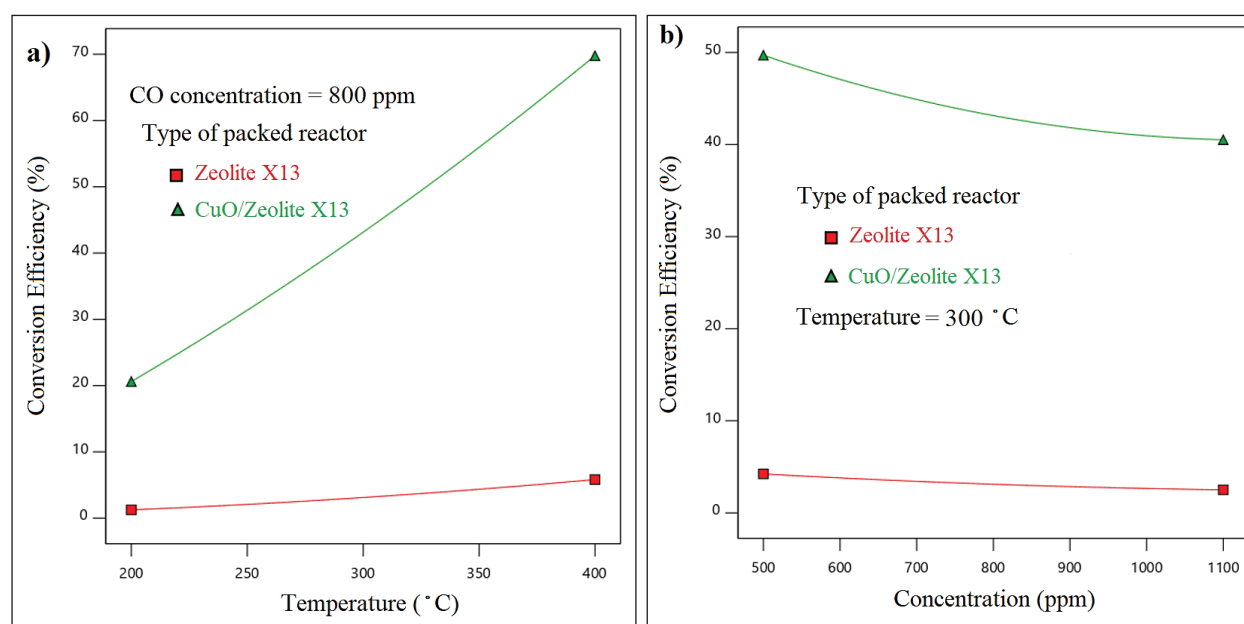


Fig. 5. The results of the effect of (a) reaction temperature and (b) carbon monoxide concentration on carbon monoxide conversion efficiency

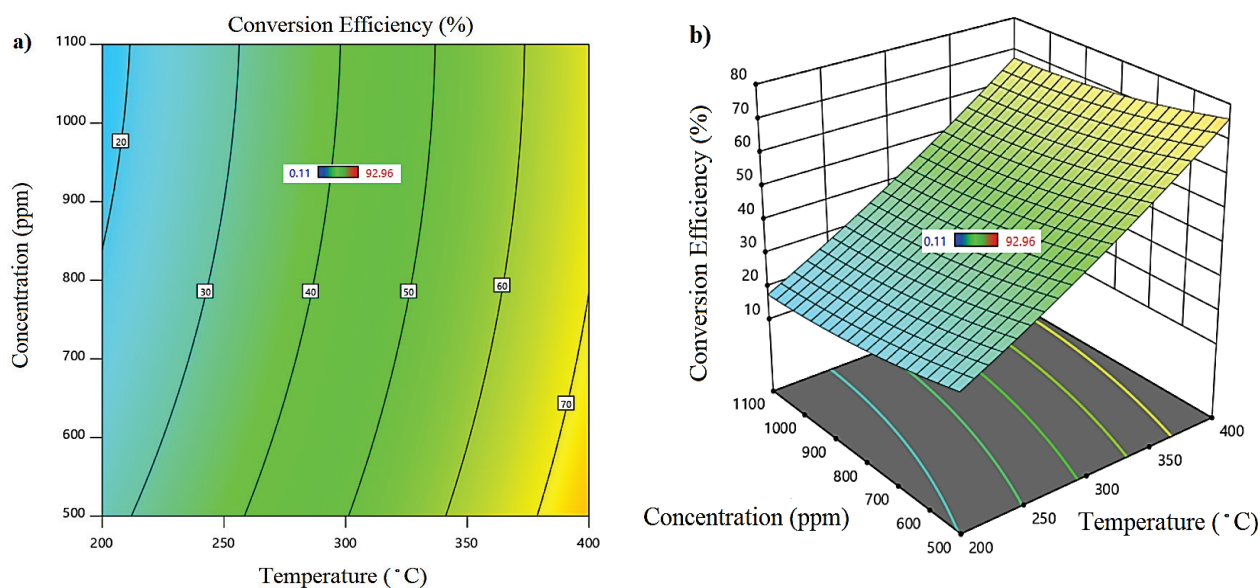


Fig. 6. a) surface view and b) three-dimensional view of the effect of main variables on carbon monoxide conversion efficiency by CuO/Zeolite 1 nanocatalyst

3.4. Three-dimensional (3D) response surfaces and contour plots

Figures 6a and 6b show three-dimensional (3D) response surfaces and contour plots indicating the main variables' effect (CO concentration and reaction temperature) on CEC by CuO/Zeolite 13X nanocatalyst. According to Figures 6a and 6b, there is a positive linear relationship between reaction temperature and CEC and a negative linear relationship between CO concentration and CEC, which means that the CEC increases with increasing temperature and decreasing CO concentration.

3.5. Determining the optimal conditions for carbon monoxide conversion efficiency and validation

In the carbon monoxide conversion process by the CuO/Zeolite 13X nanocatalyst, based on the optimization, the highest carbon monoxide conversion efficiency of 75.94% was obtained at a concentration of 500 ppm and a reaction

temperature of 400 °C as optimal conditions. Further, to confirm the correctness and validity of the model obtained from the experimental results of carbon monoxide conversion efficiency by CuO/Zeolite 13X nanocatalyst, experiments were conducted under optimal conditions, and the results are reported in Table 4. As shown in Table 4, the result of the confirmation test lies between the lower and upper limits of the 95% confidence interval, and so on, the results of predictions by the model and experimental tests are in good agreement.

3.6. Characterization of CuO/Zeolite 13X catalysts

The results of the XRF test are shown in Table 5. According to the results obtained from the XRF test, Al_2O_3 and SiO_2 , with percentages of 23.397 and 45.108, are the main components of zeolite X13, which indicates the aluminosilicate structure of this material. The structure of this article confirms this. The results of the BET test are presented in Table 6.

Table 4. Optimized conditions with predicted and experimental values for the intended response

Response	Catalyst Type	Concentration (ppm)	Temperature (°C)	Predicted Response	Confirmation Experiment	C.I (95%)	
						Low	High
CEC	CuO/Zeolite13X	500	400	75.94	82.6	68.88	82.99

Based on the results, the specific surface area and total pore volume of Zeolite 13X equal $495.85 \text{ m}^2 \text{ g}^{-1}$ and $0.265368 \text{ cm}^3 \text{ g}^{-1}$, respectively. According to the studies conducted on other types of zeolite, it was found that Zeolite 13X has a higher specific surface area compared to USY and ZSM-5 zeolite [42-44] because increasing the specific surface increases the active sites, and as a result, the reaction efficiency increases, Zeolite 13X can be a more suitable substrate for the catalyst compared to other zeolites. According to the BJH test shown in Figure 7, based on adsorption and desorption, N_2 isotherms zeolite 13X has a structure composed of mesoporous and microspores (Table 7). So 62.77% of the zeolite13X is microporous, and 37.23% is mesoporous.

The images obtained from the FE-SEM test are shown in Figure 8, and the size distribution of nanoparticles calculated using MIPCloud software is shown in Figure 9. The images presented in Figure 8 show the uniform distribution of copper oxide nanoparticles on the surface of zeolite X13. Figure 9 shows the size distribution of nanoparticles. The cumulative percentage of nanoparticle size is different; particles of 20-40 nm have the highest cumulative rate, and particles larger than 100 nm have a cumulative percentage of less than 25%. The results of the EDX test are shown in Figure 10, which shows the weight percentage of the copper element stabilized on the X13 zeolite bed. Based on the results, copper oxide nanoparticles with a weight percentage of 5.4% have been stabilized

Table 5. Elemental analysis test results(XRF) of zeolite X13

Components	Si/Al	Fe_2O_3	TiO_2	K_2O	SiO_2	Al_2O_3	MgO	Na_2O	LOI
Zeolite13X	1.928	1.027	0.017	0.504	45.108	23.397	1.92	11.336	15.95
Components	2.77	ND	ND	ND	49.28	30.17	ND	12.49	----

Table 6. Structural features of zeolite 13X (BET Equation) in CuO/Zeolite13X

Adsorption average pore diameter by BET A°	The total pore volume of pores $\text{cm}^3 \text{ g}^{-1}$	BET Surface Area m^2/g	BJH Adsorption average pore A°
21.40	0.265368	495.8508	28.172

Table 7. Characterization of microporous and mesoporous pores in CuO/Zeolite13X

Microspore volume	Microspores surface area	Mesoporous volume	Mesoporous surface area	Microspores %	Mesoporous %
0.16657	453.847	0.0988	42.003	62.77	37.23

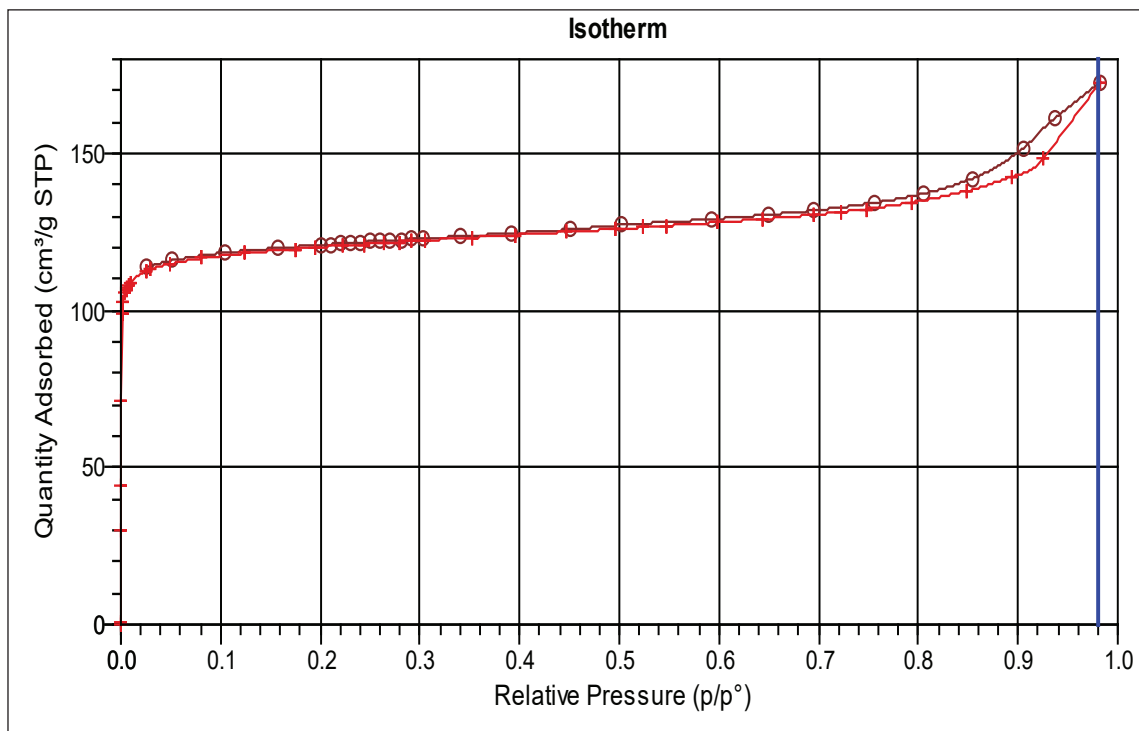


Fig. 7. Adsorption and desorption isotherms N₂ for CuO/Zeolite 13X nanocatalyst

on the X13 zeolite substrate. Based on previous studies, the optimal efficiency of carbon monoxide conversion by copper nanocatalyst with a weight percentage of 4-5% stabilized on different substrates has been reported and based on these results [20, 32], increasing the loading of copper oxide nanoparticles on the substrate does not only lead to

an increase in efficiency but also the accumulation of nanoparticles and collection of masses causes a decrease in catalytic activity. As a result of the EDX test obtained from Zeolite13X, silica and aluminum, which are the main components of zeolite, can be seen.

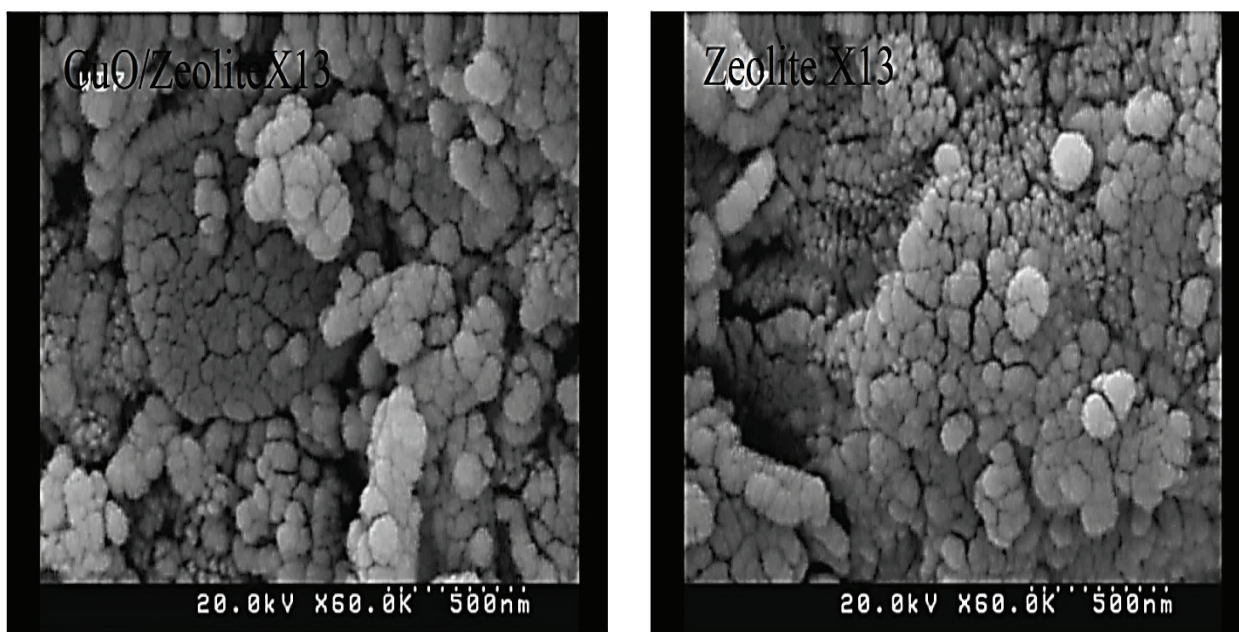


Fig. 8. Scanning electron microscope image of CuO/Zeolite 13X and zeolite 13

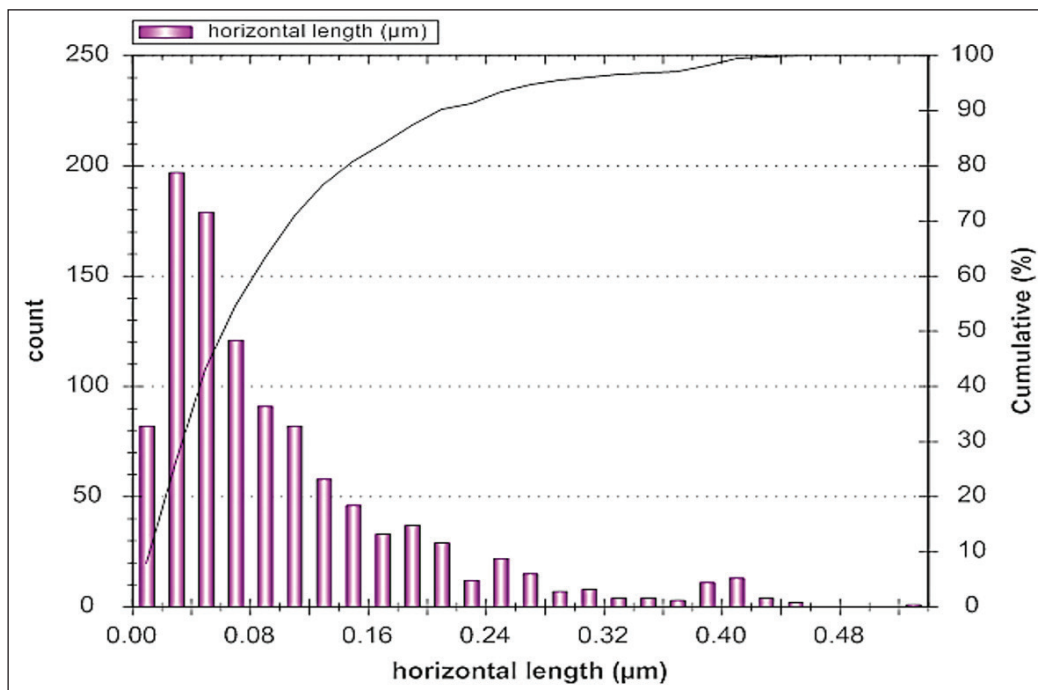


Fig. 9. Size distribution of copper oxide nanoparticles immobilized on zeolite13X

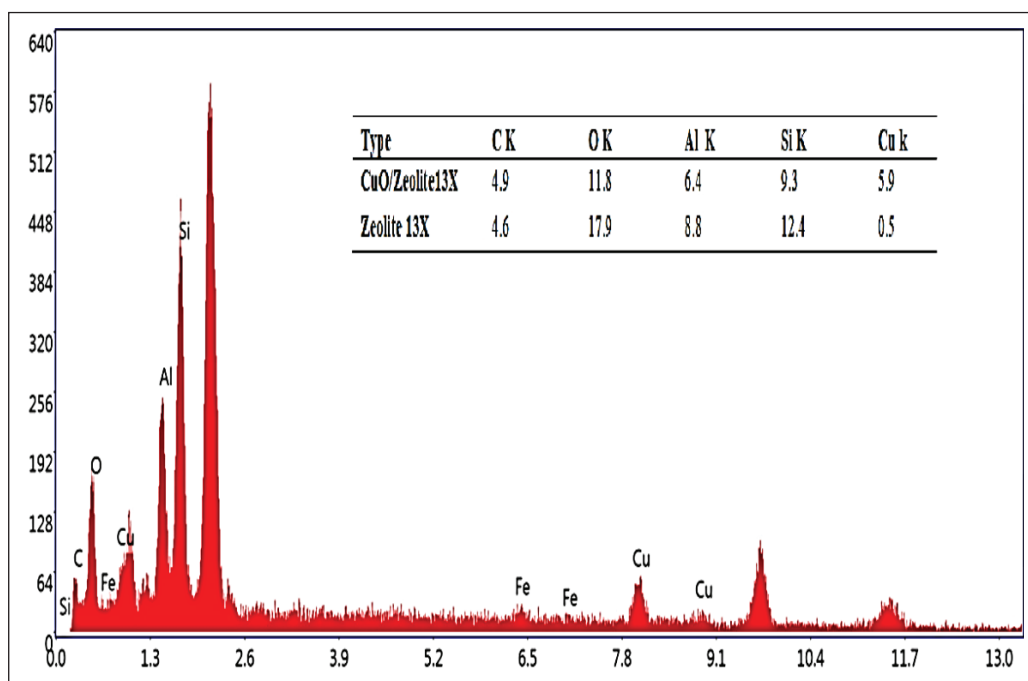


Fig. 10. Energy-dispersive X-ray spectroscopy (EDX) test results

4. Conclusion

This study was conducted to determine the efficiency of carbon monoxide conversion by CuO/Zeolite 13X nanocatalyst. Based on the results, this nanocatalyst has acceptable efficiency and thermal stability in carbon monoxide oxidation. However,

it is significant that compared to other natural and synthetic zeolites, zeolite 13X has a much higher surface area (according to the 495-bat test), which can provide many active sites for nanoparticles. However, based on the results obtained from the XRD images, it was found that the most significant

number of particles stabilized on zeolite 13X having a diameter equal to 60-40 nm, which indicates the clumping of nanoparticles and the reduction of the contact surface of the carbon monoxide flow with the nanocatalyst. Based on previous studies, nanoparticles with smaller dimensions can be produced by changing the manufacturing method, increasing efficiency and decreasing reaction temperature.

5. Acknowledgement

Dr. Hasan Asilian Mahabadi was responsible for guiding and advising on the research. Miss Bahar Parsazadeh was accountable for doing experiments, analyzing and interpreting the data, and writing the manuscript. Dr. Niloofar Damyar was responsible for data analysis, interpretation of the data, and correction of the written manuscript.

6. References

- [1] B.M. Kuehn, WHO: More than 7 million air pollution deaths each year, *Jama*, 311 (2014) 1486-1486. <https://doi.org/10.1001/jama.2014.4031>
- [2] G.K. Gulati, L.K. Gulati, S. Kumar, Carbon monoxide sensing technologies, Materials Research Forum LLC publisher, 2021. <https://www.mrforum.com/product/9781644901212/>
- [3] M. Comotti, W. C. Li, B. Spliethoff, F. Schüth, Support effect in high activity gold catalysts for CO oxidation, *J. Am. Chem. Soc.*, 128 (2006) 917–924. <https://doi.org/10.1021/ja0561441>
- [4] A. Joneydi Jaffari, M.J. Asari, M. Saremi, Determination of some air pollutants emitted from hospital incinerators in Hamadan in 2002, *J. Maz. Univ. Med. Sci.*, 15 (2005) 95-102. <http://jmums.mazums.ac.ir/article-1-797-en.html>
- [5] G. Goudarzi, An assessment on dispersion of carbon monoxide from acement factory, *J. Environ. Health Manage. Eng.*, 3 (2017) 163-168. <http://eprints.kmu.ac.ir/id/eprint/26577>
- [6] F. Golbabaee, A. Vahid, A. Faghihi Zarandi, A novel nano-palladium embedded on the mesoporous silica nanoparticles for mercury vapor removal from air by the gas field separation consolidation process, *Appl. Nanosci.*, 12 (2022) 1667-1682. <https://doi.org/10.1007/s13204-022-02366-0>
- [7] S. Royer, D. Duprez, Catalytic oxidation of carbon monoxide over transition metal oxides, *Chem. Cat. Chem.*, 3 (2011) 24-65. <https://doi.org/10.1002/cctc.201000378>
- [8] R.M. Heck, R.J. Farrauto, S.T. Gulati, Catalytic air pollution control: commercial technology, 3rd edition, John Wiley & Sons publisher, 544 pages, 2012. <https://onlinelibrary.wiley.com/>
- [9] M.D. Mobarake, Thiol modified bimodal mesoporous silica nanoparticles for removal and determination toxic vanadium from air and human biological samples in petrochemical workers, *NanoImpact*, 23 (2021)100339. <https://doi.org/10.1016/j.impact.2021.100339>
- [10] L. Theodore, Air pollution control equipment calculations, John Wiley & Sons, 2008. <https://doi.org/10.1002/9780470255773>
- [11] M. Chen, Highly active surfaces for CO oxidation on Rh, Pd, and Pt, *Surf. Sci.*, 601(2007) 5326-5331. <https://doi.org/10.1016/j.susc.2007.08.019>
- [12] G. Ertl, Reactions at surfaces: From atoms to complexity (Nobel lecture), *Angewandte Chem. Int. Edit.*, 47 (2008) 3524-3535. <https://doi.org/10.1002/anie.200800480>
- [13] S. Dey, Cobalt doped CuMnOx catalysts for the preferential oxidation of carbon monoxide, *Appl. Surf. Sci.*, 2441(2018) 303-316. <https://doi.org/10.1016/j.apsusc.2018.02.048>
- [14] H. Yen, Tailored mesostructured copper/ceria catalysts with enhanced performance for preferential oxidation of CO at low temperature, *Angewandte Chem.*, 124 (2012) 12198-12201. <https://doi.org/10.1002/ange.201206505>
- [15] M. Krämer, Structural and catalytic aspects of sol-gel derived copper manganese oxides as low-temperature CO oxidation catalyst, *Appl. Catal. A: General*, 302 (2006) 257-263. <https://doi.org/10.1016/j.apcata.2006.01.018>

- [16] M.G. Jeong, Room temperature CO oxidation catalyzed by NiO particles on mesoporous SiO₂ prepared via atomic layer deposition: Influence of pre-annealing temperature on catalytic activity, *J. Mol. Catal. A: Chem.*, 414 (2016) 87-93. <https://doi.org/10.1016/j.molcata.2016.01.002>
- [17] J. Knudsen, Low-temperature CO oxidation on Ni (111) and on a Au/Ni (111) surface alloy, *ACS Nano*, 4 (2010) 4380-4387. <https://doi.org/10.1021/nn101241c>
- [18] Q. Guo, Y. Liu, MnOx modified Co₃O₄-CeO₂ catalysts for the preferential oxidation of CO in H₂-rich gases, *Appl. Catal. B: Environ.*, 82 (2008) 19-26. <https://doi.org/10.1016/j.apcatb.2008.01.007>
- [19] D. Svintsitskiy, Low-temperature catalytic CO oxidation over mixed silver-copper oxide Ag₂Cu₂O₃, *Appl. Catal. A: General*, 510 (2016) 64-73. <https://doi.org/10.1016/j.apcata.2015.11.011>
- [20] M. Kikugawa, K. Yamazaki, H. Shinjoh, Characterization and catalytic activity of CuO/TiO₂-ZrO₂ for low temperature CO oxidation, *Appl. Catal. A: General*, 547 (2017) 199-204. <https://doi.org/10.1016/j.apcata.2017.09.005>
- [21] J.A. Schwarz, C.I. Contescu, K. Putyera, Dekker encyclopedia of nanoscience and nanotechnology, CRC press, Vol 5, 4014 pages, 2004. <https://www.routledge.com/go/crc-press>
- [22] A.F. Zarandi, P. Paydar, A novel method based on functionalized bimodal mesoporous silica nanoparticles for efficient removal of lead aerosols pollution from air by solid-liquid gas-phase extraction, *J. Environ. Health Sci. Eng.*, 18 (2020) 177-188. <https://doi.org/10.1007/s40201-020-00450-7>
- [23] B. Solsona, Total oxidation of VOCs on mesoporous iron oxide catalysts: Soft chemistry route versus hard template method, *Chem. Eng. J.*, 290 (2016) 273-281. <https://doi.org/10.1016/j.cej.2015.12.109>
- [24] J. Kašpar, P. Fornasiero, N. Hickey, Automotive catalytic converters: current status and some perspectives, *Catal. Today*, 77 (2003) 419-449. [https://doi.org/10.1016/S0920-5861\(02\)00384-X](https://doi.org/10.1016/S0920-5861(02)00384-X)
- [25] M. Bandyopadhyay, Gold nano-particles stabilized in mesoporous MCM-48 as active CO-oxidation catalyst, *Micropor. Mesopor. Mater.*, 89 (2006) 158-163. <https://doi.org/10.1016/j.micromeso.2005.09.029>
- [26] C.W. Chiang, A. Wang, C.-Y. Mou, CO oxidation catalyzed by gold nanoparticles confined in mesoporous aluminosilicate Al-SBA-15: Pretreatment methods, *Catal. Today*, 117 (2006) 220-227. <https://doi.org/10.1016/j.cattod.2006.05.026>
- [27] Y. Jing, Preparation, Characterization and catalytic oxidation property of CeO₂/Cu²⁺-attapulgite (ATP) nanocomposites, *J. Rare Earths*, 28 (2010) 347-352. [https://doi.org/10.1016/S1002-0721\(10\)60328-6](https://doi.org/10.1016/S1002-0721(10)60328-6)
- [28] M. Moshoeshe, M. S. Nadiye-Tabbiruka, V. Obuseng, A review of the chemistry, structure, properties and applications of zeolites, *Am. J. Mater. Sci.*, 7 (2017) 196-221. <https://doi.org/10.5923/j.materials.20170705.12>
- [29] I. Petrov, T. Michalev, Synthesis of zeolite A: a review, *Sci. Works Ruse Univ.*, 51(2012) 30-35. <https://www.scribd.com/document/435962390/Synthesis-of-Zeolite-a-a-Review>
- [30] G. Busca, Heterogeneous catalytic materials, solid state chemistry, surface chemistry and catalytic behaviour, 1st Edition, Elsevier, 2014. <https://shop.elsevier.com/books/heterogeneous-catalytic-materials/busca/978-0-444-59524-9>
- [31] M. Arjomandi, A review of analytical methods, *Anal. Methods in Environ. Chem. J.*, 2 (2019) 97-126. <https://doi.org/10.24200/amecj.v2.i03.73>
- [32] S. D. Athar, H. Asilian, Catalytic Oxidation of Carbon Monoxide Using Copper-Zinc Mixed Oxide Nanoparticles Supported on Diatomite, *J. Health Scope*, 1 (2012) 52-56. <https://doi.org/10.24200/amecj.v2.i03.7310.5812/jhs.4590>

- [33] F. Mansouri, Energy efficiency improvement in nitric oxide reduction by packed DBD plasma: optimization and modeling using response surface methodology (RSM), *Environ. Sci. Pollut. Res.*, 27 (2020) 16100-16109. <https://doi.org/10.1007/s11356-020-07870-w>
- [34] N. Hasyimah, M. Rashid, H. Norelyza, Optimization of a developed multi-cyclone using response surface methodology (RSM) to control fine particulate emission, *Eng. Innov.*, 4 (2023) 21-29. <https://doi.org/10.4028/p-7540tu>
- [35] A.N. Tamar, M. Karbasi, M. R. Khani, Response surface methodology (RSM) for optimizing ozone-assisted process parameters for formaldehyde removal, *J. Environ. Health Sci. Eng.*, 21 (2023) 475-484. <https://doi.org/10.1007/s40201-023-00873-y>
- [36] R.M. Gholami, S. Mousavi, and S. Borghei, Process optimization and modeling of heavy metals extraction from a molybdenum rich spent catalyst by *Aspergillus niger* using response surface methodology, *J. Ind. Eng. Chem.*, 18 (2012) 218-224. <https://doi.org/10.1016/j.jiec.2011.11.006>
- [37] M. Fayazi, Removal of Safranin dye from aqueous solution using magnetic mesoporous clay: optimization study, *J. Mol. Liq.*, 212 (2015) 675-685. <https://doi.org/10.1016/j.molliq.2015.09.045>
- [38] W. Djoudi, F. Aissani-Benissad, S. Bourouina-Bacha, Optimization of copper cementation process by iron using central composite design experiments, *Chem. Eng. J.*, 133 (2007) 1-6. <https://doi.org/10.1016/j.cej.2007.01.033>
- [39] B. White, Complete CO oxidation over Cu₂O nanoparticles supported on silica gel, *Nano Lett.*, 6 (2006) 2095-2098. <https://doi.org/10.1021/nl061457v>
- [40] C.Y. Lu, M. Y. Wey, The performance of CNT as catalyst support on CO oxidation at low temperature, *Fuel*, 86 (2007) 1153-1161. <https://doi.org/10.1016/j.fuel.2006.09.022>